JOURNAL OF Applied Polymer SCIENCE

Preparation and Properties of MWCNTs/Poly(Acrylonitrile-Styrene-Butadiene)/Epoxy Hybrid Composites

Jyotishkumar P,[1] Eldho Abraham,[2] Sajeev Martin George,[1] Eldho Elias,[1] Jürgen Pionteck,[3] Paula Moldenaers,[4] Sabu Thomas[1,5,6,7]

[1]School of Chemical Sciences, Mahatma Gandhi University, Priyadarshini Hills, Kottayam, Kerala 686560, India
[2]Department of Chemistry, Bishop Moore College, Mavelikkara, Kerala, 690110, India
[3]Department of Polymer Reactions and Blends, Leibniz Institute of Polymer Research Dresden, 01069 Dresden, Germany
[4]Department of Chemical Engineering, Catholic University of Leuven, de Croylaan 46, B-3001, Leuven, Belgium
[5]Centre for Nanoscience and Nanotechnology, Mahatma Gandhi University, Priyadarshini Hills, Kottayam, Kerala 686560, India
[6]Faculty of Applied Sciences, Universiti Teknologi MARA, 40450 Shah Alam Selongor, Malaysia
[7]Center of Excellence for Polymer Materials and Technologies, Tehnoloski park 24, 1000 Ljubljana, Slovenia
Correspondence to: S. Thomas (E-mail: sabupolymer@yahoo.com)

ABSTRACT: Poly(acrylonitrile-styrene-butadiene) (ABS) was used to modify diglycidyl ether of bisphenol-A (DGEBA) type epoxy resin, and the modified epoxy resin was used as the matrix for making multiwaled carbon tubes (MWCNTs) reinforced composites and were cured with diamino diphenyl sulfone (DDS) for better mechanical and thermal properties. The samples were characterized by using infrared spectroscopy, pressure volume temperature analyzer (PVT), thermogravimetric analyzer (TGA), dynamic mechanical analyzer (DMA), thermo mechanical analyzer (TMA), universal testing machine (UTM), and scanning electron microscopy (SEM). Infrared spectroscopy was employed to follow the curing progress in epoxy blend and hybrid composites by determining the decrease of the band intensity due to the epoxide groups. Thermal and dimensional stability was not much affected by the addition of MWCNTs. The hybrid composite induces a significant increase in both impact strength (45%) and fracture toughness (56%) of the epoxy matrix. Field emission scanning electron micrographs (FESEM) of fractured surfaces were examined to understand the toughening mechanism. FESEM micrographs reveal a synergetic effect of both ABS and MWCNTs on the toughness of brittle epoxy matrix.

KEYWORDS: hybrid composites; volume shrinkage; thermal and mechanical properties; electron micrographs

Received 22 November 2011; accepted 27 February 2012; published online
DOI: 10.1002/app.37677

INTRODUCTION

Epoxy resins are widely used in industrial applications, as construction materials, in automobile industry, aerospace applications, adhesives, coatings, electronic circuit board laminates, etc. due to their good stiffness, low shrinkage, dimensional stability, good chemical and water resistance, low cost, ease of processing, fine adhesion to many substrates, low specific weight, and long pot life period.[1–4] However, cured epoxy resins have low toughness and poor crack resistance that prevent their wider applications. The most common method to increase the fracture toughness is the incorporation of rubber that separates from the matrix during curing, leading to different morphologies.[5–7] The advantage of rubber toughening in thermosets is that fracture toughness can be improved. Here, the dispersed rubber prevents the crack propagation and there by enhances the toughness. However, rubber modification will lead to significant reduction in the modulus and thermal stability of the material. Recently, many attempts have been made to toughen thermosetting resins with high performance thermoplastics,[8–10] because of their high modulus and glass transition temperatures. Different types of thermoplastics have been used to modify epoxy resin such as poly-ether-sulfone, poly-ether-imide, poly(acrylonitrile-styrene-butadiene) (ABS), etc.[11–14] The final properties of epoxy blends greatly depend on final morphology of the polymer blends, which depends on the selection of the thermoplastic polymer, content of thermoplastic, the epoxy precursors, the hardener, and the curing temperature.[15]

A new approach aiming to overcome this basic problem is related to nanotechnology and uses of fillers in the nanometer scale. Recently, many researchers showed that addition of nano

fillers not only increase the toughness but also strengthen the obtained composites.[16–19] The discovery of carbon nanotubes and carbon nanostructured materials has inspired scientists to develop advanced materials for a range of potential applications because of their high aspect ratio, low density, and their exceptional physical properties (electrical, thermal, and mechanical).[19–23] CNT have already been employed for devices ranging from loud speakers, solar cells, high-reliability touch screens, flexible displays, etc.[24–26] Different polymer multiwalled carbon nanotubes (MWCNTs) composites have been synthesized by incorporating MWCNTs into various polymer matrices, such as polyamides, polyimides, epoxy resins, polyurethane, and polypropylene.[19,27–31] These polymers based on nanocomposites gain their high properties, particularly mechanical properties, at low filler content owing to the high aspect ratio and high surface area to the volume ratio of the nano-sized particles.

Recently, researches were inspired by the new concept "hybrid composites" for improved toughness. There were few studies already reported based on the concept of hybrid composites. For instance, the simultaneous addition of clay and rubber in epoxy resin,[32] addition of clay and core shell rubber particles in epoxy resin,[33] addition of clay and PMMA in epoxy resin,[34,35] addition of nano silica, and CTBN in epoxy resin.[36] Such materials are often referred to as hybrid composites because they contain both soft and hard particles. According to the literature, a synergetic effect in toughness was observed in hybrid composites. Current research is directed toward the use of both ABS and MWCNTs in an epoxy-amine system to achieve enhanced toughness.

The curing kinetics, phase separation, volume shrinkage, thermal and mechanical properties of ABS/epoxy blends, and epoxy/MWCNTs composites have been discussed in detail in our previous studies.[4,14,37,38] It has been proved that 3.6 wt % ABS/epoxy blend possesses superior mechanical and thermal properties compared to the other blends. The main objective of this study is to explore the effect of MWCNTs loading in 3.6 wt % ABS/epoxy blend matrix. The cure behaviour, volume shrinkage, thermal, mechanical, and morphological properties of the hybrid composites were investigated as a function of MWCNTs composition. The relationship between morphology and the thermo-mechanical properties of hybrid composites has been discussed. Further, the toughening mechanism was also investigated in detail. The resulting hybrid composites were found to have superior toughness while retaining the thermo-mechanical properties of the epoxy blend and neat crosslinked epoxy.

EXPERIMENTAL SECTION

Materials

The matrix material used in the experiments consists of diglycidyl ether of bisphenol-A (DGEBA) (Lapox L-12, Atul, India) and 4,4′-diamino diphenyl sulfone (DDS) (Lapox K-10, Atul). The toughener ABS (Poly lac PA-757K) was manufactured by Chi Mei Corporation, Taiwan. The used poly (acrylonitrile-butadiene-styrene) (ABS) is a commercially available thermoplastic polymer consisting of 70 wt % polystyrene (PS), 25 wt % acrylonitrile, and 5 wt % agglomerated polybutadiene. The molecular weight of the soluble part of ABS was determined to be M_n = 51300 g/mol and M_w = 125200 g/mol (PDI = 2,44, GPC, PS standard), and the density was determined to be 1.051 g/cm^3 by means of an Helium Pycnometer. The used MWCNTs (Baytube® 150P) was procured from Bayer Material Science AG (Leverkusen, Germany) synthesised by catalytic carbon vapour disposition process. Baytubes have purity >95 % and an average diameter 13–16 nm with length >1 μm.

Preparation of Hybrid Composites

Blend of epoxy resin/ABS containing 3.6 wt % ABS were prepared using the melt mixing technique. ABS was mixed with epoxy resin at 180°C under constant stirring. After proper mixing, MWCNTs were dispersed in the blend and mixed at 180°C using a sonicator for 15 min. In a second step, DDS was added to MWCNTs/epoxy blend mixture with an epoxy:amine ratio of 2 : 1. After dissolving the DDS in MWCNTs/ABS/epoxy resin solution, the composites were cured in an air oven for 3 h at 180°C followed by postcuring at 200°C for 2 h. Composites with MWCNTs content 0.1, 0.3, and 0.5 g in the ABS/epoxy-hardener mixture (100 g DGEBA + 5 g ABS + 35 g DDS) were prepared, and the samples were named according to the final MWCNTs concentration as 0.07 wt % MWCNTs, 0.21 wt % MWCNTs, and 0.36 wt % MWCNTs. (For comparison, a sample without ABS and MWCNTs, named as neat epoxy, and a sample with ABS only, named as epoxy blend, were prepared.)

For Fourier transform infrared spectrometer (FTIR), differential scanning calorimetry (DSC), and pressure-volume-temperature (PVT) observations, the freshly prepared mixtures were immediately used or stored before use in a freezer at −20°C. For other experiments, the freshly prepared mixtures were cured in the air oven at 180°C for 3 h and then postcured at 200°C for further 2 h. The resultant composites were then allowed to cool slowly to room temperature.

CHARACTERIZATION TECHNIQUES

Fourier Transform Infrared Spectrometry

In situ curing studies were carried out by using Infrared Fourier spectrometer EQUINOX 55 (Bruker Optik GmbH). A few milligrams of sample are placed in a sample holder, and *in situ* FTIR was run at 150°C for 3 h. Please note that at 180°C, the reaction between epoxy and amine is too fast to be followed by *in situ* FTIR analysis.

Pressure-Volume-Temperature Analysis

The pressure-volume-temperature (PVT) measurements were done using a fully automated GNOMIX high pressure mercury dilatometer. Below 200°C, the absolute accuracy of the instrument is of 0.002 cm^3/g. In practice, the change in specific volume is small as 0.0002 cm^3/g can be resolved reliably. The crosslinking reaction was characterized in the so-called data acquisition mode at 10 MPa and 180°C by following the volume shrinkage of the samples as a function of time. To check whether any crosslinking has taken place during the sample preparation stages, the experimental initial specific volumes were compared with those calculated initial specific volumes from the densities of the individual components by assuming an additive behavior (Table I). The lower values for

Table I. Experimental and Calculated Initial Specific Volume for Neat Epoxy, Blend, and Hybrid Composite at 180°C

Specimen	Specific volume experimental (V_{EO})	Specific volume calculated (V_{TO})
Neat epoxy	0.8926	0.9000
Epoxy blend	0.8934	0.9037
0.36 wt % MWCNTs hybrid composites	0.8965	0.9018

experimental specific volumes indicate a certain degree of crosslinking; however, the deviation was within the acceptable range (1%).

Thermogravimetric Analysis

Thermal stability of the hybrid composites was analyzed by thermogravimetric analyzer (TGA). TA instrument TGA Q 5000 was used to monitor the degradation. The measurements were performed on 3–5 mg of the samples from room temperature (25°C) to 800°C/min at a heating rate of 10 K/min and under nitrogen atmosphere.

Dynamic Mechanical Analysis

The investigation of thermo mechanical behavior properties was performed using TA instruments DMA 2980 dynamic mechanical thermal analyzer. Rectangular specimens of 40 × 10 × 3 mm^3 were used for the analysis. The analysis was done in single cantilever mode at a frequency of 1 Hz, from −100 to 300°C and at a heating rate of 1 K/min.

Thermo Mechanical Analysis

The thermomechanical properties of neat epoxy, epoxy blend, and hybrid composites were measured using a TA instrument Q 400, thermo mechanical analyser. The samples were scanned from 50 to 250°C at a heating rate of 1 K/min. Rectangular specimens of 20 × 10 × 3 mm^3 were used for the analysis.

Impact Strength

Charpy impact strength of the unmodified and modified epoxy resin was measured following the specifications ISO 179/1eA. Impact tests were performed on Zorn Stendal impact testing machine. The dimensions of the specimens were approximately 40 × 8 × 4 mm^3.

Fracture Toughness

Fracture toughness of the specimens was determined according to ASTM D 5045-99. The measurements were taken with a universal testing machine Zwick (UPM - Z010). The material is taken in the form of rectangular sheet, the specimen thickness, $d = 4$ mm was taken, and it is identical with the sheet thickness. The sample width, $b = 2d$. In the specimen geometry, the crack length, a, is selected in such a way that $0.45 < a/b < 0.55$. The analysis was done in bending mode at room temperature. The value of (K_{Ic}) was calculated using eq. (1).

$$\text{Stress intensity factor}, K_{Ic} = \frac{QPa^{1/2}}{bd} \quad (1)$$

where P is the load at the initiation of crack, a is the crack length, b is the breadth of the specimen, d is the thickness of the specimen, and Q is geometry constant. Q is calculated using the following equation,

$$Q = 1.99 - 0.41(a/b) + 18.7(a/b)^2 - 38.48(a/b)^3 + 53.85(a/b)^4 \quad (2)$$

Field emission Scanning Electron Microscopy

The morphology of fractured surface of crosslinked epoxy composites were examined using a ULTRA field emission scanning electron microscopy (FESEM) (model ULTRA plus, Carl Zeiss NTS GmbH, Germany). The samples were coated with platinum by vapor deposition using a SCD 500 Sputter Coater (BAL-TEC AG, Liechtenstein).

RESULTS AND DISCUSSION

Spectroscopic Analysis

Figure 1(a) shows the FTIR spectra of 0.36 wt % MWCNTs-modified hybrid epoxy composites, which is a represent of all

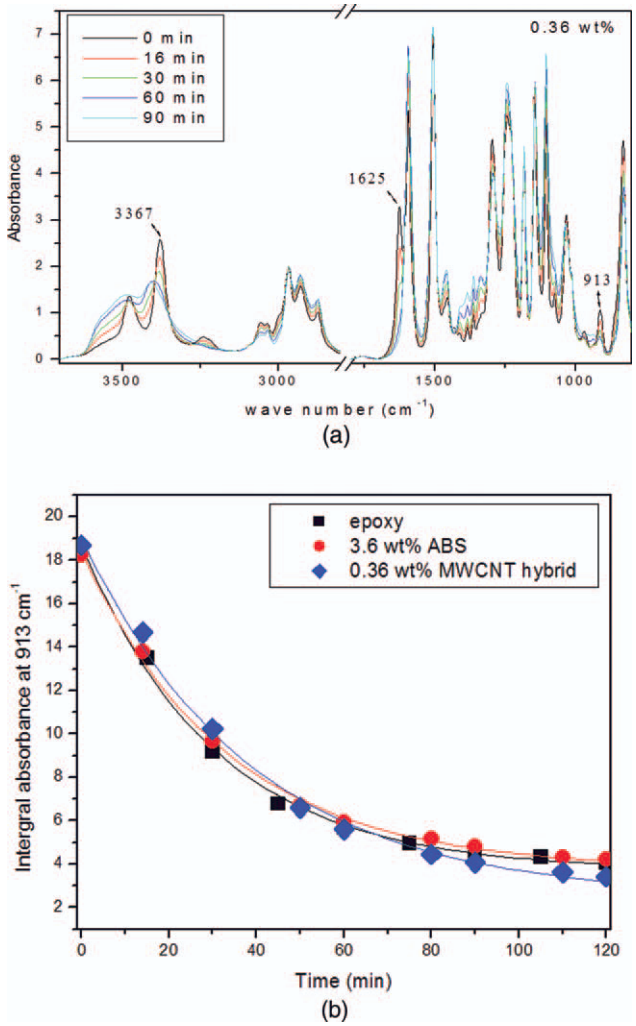

Figure 1. (a) FTIR spectra for 0.36 wt % MWCNTs/ABS/epoxy hybrid nanocomposite. (b) Exponential decay behavior of epoxy resin in epoxy/amine mixture during curing (lines are the fitted curves). [Color figure can be viewed in the online issue, which is available at wileyonlinelibrary.com.]

Table II. First-Order Decay Constants for ABS Modified Epoxy Blends

Specimen	T_1	Y_0	A_1	R^2
Neat epoxy	30.42 ± 1.81	3.71 ± 0.24	15.04 ± 0.34	0.997
3.6 wt % ABS	32.99 ± 1.65	3.75 ± 0.20	14.68 ± 0.27	0.998
Hybrid composite	38.40 ± 3.10	2.48 ± 0.41	16.57 ± 0.47	0.996

the composites studied. From the figure, the intense signal of the epoxy ring is centered at 913/cm due to the asymmetrical ring stretching, in which the C—C bond stretches during the contraction of the C—O bond.[39] The epoxide band at 913/cm is very evident at the beginning of the experiment ($t = 0$), gradually disappears with curing time and almost is not detectable after 90 min, indicating the time for the consumption of epoxide groups. On the other hand, the strong absorbances at 1625 and 3367/cm of the NH_2 groups from the DDS also reduce with curing time and almost disappear after 90 min, again indicating the time for complete epoxy/amine conversion. However, during polymerization, the spectrum between 3100 and 3600 becomes complex, and the unreacted amines and hydroxyl groups overlap to a broad band and the absorbance at 1625/cm forms after short curing time a shoulder to the strong absorption at 1594/cm caused by phenyl ring.[40] Therefore, the rate of epoxy/amine polymerization can be estimated by following the loss of epoxy band intensity with respect to cure time. In Figure 1(b), we compare the loss of epoxide band with respect to cure time for all the composites studied by FTIR. We observe similar behavior for all the systems studied that is a rapid decrease of epoxide band intensity within the first 45 min followed by a slow decrease in the next hour. However, the band does not completely disappear and the intensity levels off.

To evaluate the cure reaction more detailed, the loss of epoxide band with respect to cure time was simulated with Maxwells equation.

$$y = y_0 + A_1 \exp(-x/t_1) \tag{3}$$

As $t = \alpha$, $y = y_0$. Here, A_1 is the magnifier and t_1 is the reaction time of the cure reaction and could indicate the rate of the reaction in blends and composites. As shown in Figure 1(b), the simulation results gave a good fit to the experimental data. The fit parameters, t_1, A_1, y_0, and R^2 to assess the quality of fit are given in Table II. The decay time t_1 increases with filler addition due to the decrease in rate of the epoxy/amine reaction by the presence of ABS and MWCNTs. In blends, the presence of ABS dilutes the epoxy-DDS reaction volume and hence progressively decreases the rate of epoxy/amine reaction.[4] On the other hand, in hybrid composites, dispersed MWCNTs can act as a physical hindrance to the mobility of monomers and lower mobility of monomer may reduce the rate of epoxy/amine reaction; off course dilution effect of ABS cannot be neglected.[41,42]

Pressure Volume Temperature Studies

Pressure-volume-temperature characterization is a well-known tool for the investigation of the change in specific volume with respect to cure time for epoxy systems. Figure 2(a) gives the change in specific volume data obtained for neat epoxy, blend, and 0.36 wt % MWCNTs/ABS/epoxy hybrid composites with respect to cure time. A temperature of 180°C and a pressure of

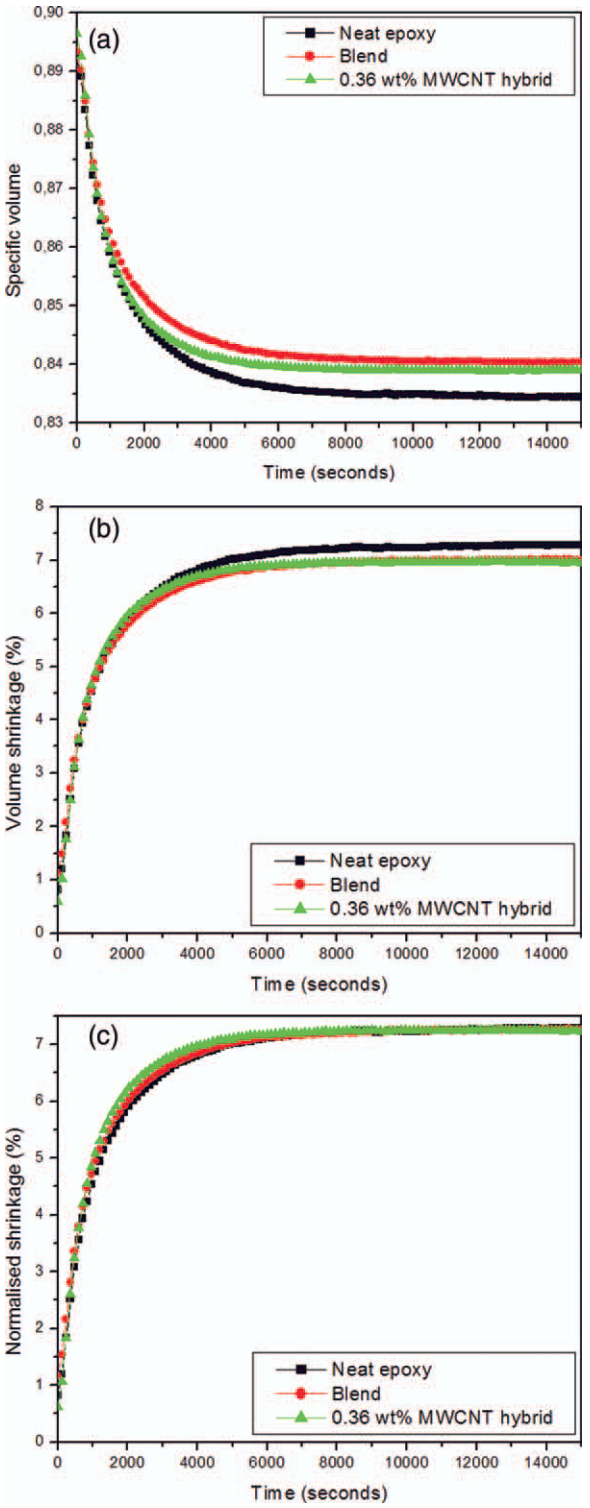

Figure 2. (a) Specific volume versus curing time for PVT test at 180°C. (b) Volume shrinkage versus curing time for PVT test at 180°C. (c) Normalized shrinkage versus curing time for PVT test at 180°C.

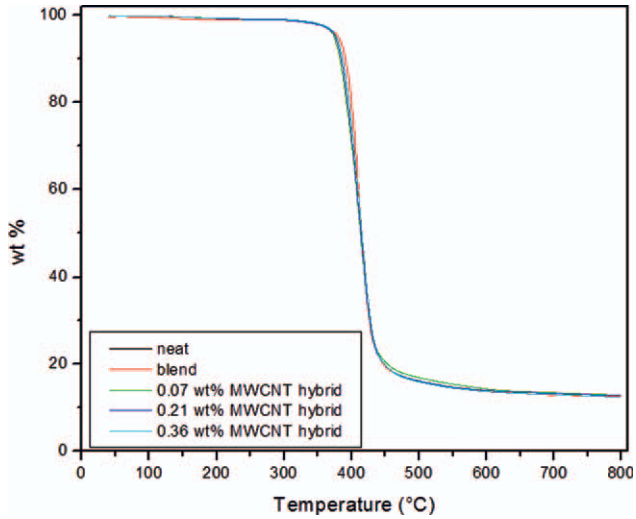

Figure 3. TGA of neat epoxy, blend, and hybrid composites.

10 MPa were applied for 13 h, during which a sharp decrease in the specific volume was observed for both epoxy blend and hybrid composite due to the *in situ* epoxy-amine reaction (volume shrinkage).[4] After heating for 2 h, the specific volume reached an almost constant value for composites. The absolute specific volume increases with lower density thermoplastic content. The beginning of the final plateau region corresponds to the vitrification process; although at this stage, the curing reaction could continue slowly.

From the specific volume values, the percentage volume shrinkage of the composites at any time t could be calculated as

$$(\Delta V) = ((V_{T0} - V_E)/V_{T0}) \times 100 \quad (4)$$

where VT_0 is the theoretical specific volume of the composites at time $t = 0$ and V_E is the experimental specific volume for the composites at any time t. Since epoxy is the matrix material, the measured volume shrinkage is always the shrinkage of the epoxy phase. From Figure 2(b), there is not much influence of MWCNTs on volume shrinkage of the epoxy phase has been observed. However, in our previous study, we observe a profound influence of MWCNTs on the volume shrinkage of the epoxy phase due to generation of constrained epoxy polymer layers around the filler surface. The influence of MWCNTs may be overlapped by the presence of ABS in the hybrid composites.

Furthermore, we have calculated the normalized shrinkage, (ΔV_N) with respect to the epoxy volume content in the composite using the eq. (5).[4]

$$(\Delta V_N) = (\Delta V)/\text{wt \% of epoxy phase}) \times 100 \quad (5)$$

Figure 2(c) reveals normalized shrinkage values as a function of the MWCNTs content; again, the % normalized shrinkage remains comparable for MWCNTs hybrid composites with respect to neat epoxy and epoxy blend. Again supporting the fact that both ABS and MWCNTs have not much influence on the % shrinkage of epoxy phase.

Thermogravimetric Analysis

Thermal stability of neat epoxy, epoxy blend, and hybrid composites were studied by thermogravimetric analysis (TGA) in nitrogen atmosphere. The TGA curves for all the composites are

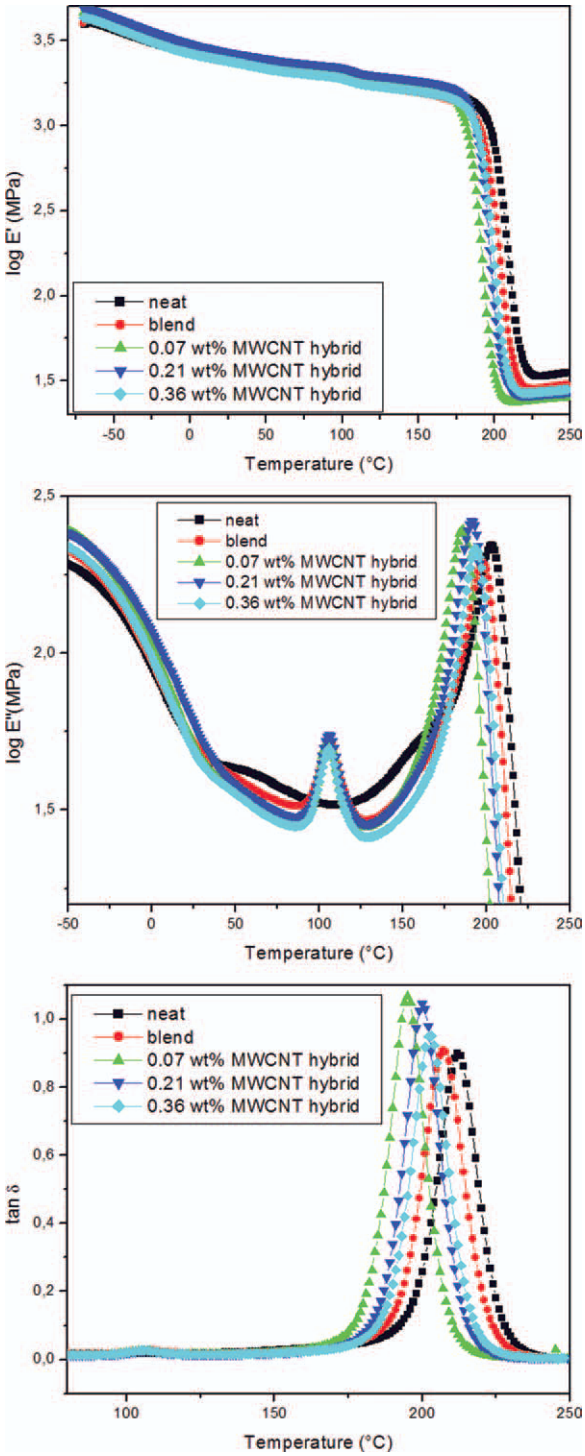

Figure 4. (a) Log E′ versus temperature plot for neat epoxy, blend, and hybrid composites. (b) Log E″ versus temperature plot for neat epoxy, blend, and hybrid composites. (c) Tan δ versus temperature plot for neat epoxy, blend, and hybrid composites.

Table III. Parameters Obtained From Tan δ Profile

Materials	Tan δ peak height	Tan δ peak width at half height	Tan δ peak area	Tan δ peak (°C)	M_c (g/mol)	$\upsilon_e \times 10^{27}$ (chains/m^3)
Neat	0.89	16	17.88	212	322.31	2.24
Blend	0.90	16	17.92	207	336.20	2.15
0.07 wt %	1.07	14	19.03	195	375.00	1.93
0.21 wt %	1.04	14	18.05	200	357.79	2.02
0.36 wt %	0.95	15	17.67	203	348.21	2.07

given in Figure 3. There is no deterioration in thermal stability of the hybrid composite as compared with that of the neat material. Thermal stability can be expressed in terms of parameters like initial decomposition temperature, final degradation temperature, and final residue.[43] From the graph, it is clear that the initial decomposition temperature (T_i), final degradation temperature (T_{max}), and residual weight fraction for all the composites remain the same at various temperatures indicating that the thermal stability of cured epoxy blends was not affected by the addition of MWCNTs. The average weight loss of around 1–2% up to 300°C is due to the release of moisture. On the other hand, the weight loss above 350°C is related to the decomposition of the polymer.[43]

Dynamic Mechanical Analysis

Dynamic storage modulus (E') measures the load bearing capacity of a composite material. The log storage modulus ($log\ E'$) recorded as a function of temperature for unmodified and modified epoxy resin, is shown in Figure 4(a). The $log\ E'$ of the MWCNTs hybrid composites were found to be higher than neat materials below the glass transition region (T_g). This may be due to the increase in the stiffness of the matrix with the reinforcement effect imparted by the MWCNTs.[43] After the T_g modulus decreases due to the segmental motion of the polymer chains. The storage modulus of the hybrid composites in the rubbery region was slightly less than neat materials. Also, storage modulus in the rubbery region is an indirect measure of crosslink density.[44] The lower value of storage modulus in this region indicates that the crosslink density of the hybrid composites is low. In this case, lower crosslink density of the blend and hybrid composites with respect to neat epoxy is well understood from the decrease in T_g of the epoxy phase (spectra of storage modulus). The presence of ABS and MWCNTs in the hybrid composites hinders the curing reaction of epoxy resin with amine due to the dilution effect of ABS phase and MWCNTs–epoxy interactions, which decreases the T_g of epoxy rich phase.

Loss modulus (E'') is a measure of the viscous response of the material. The log of loss modulus (E'') is recorded as a function of temperature for all the system studied and is shown in Figure 4(b). From the Figure, blends and hybrid composites exhibit two transition peaks corresponding to SAN rich phase and epoxy rich phase, respectively. The peak at lower temperature is due to thermoplastic rich phase and that at higher temperature is due to the epoxy rich phase.[45] There is a shift in the epoxy T_g toward the lower temperatures on increasing the MWCNTs content due to the hindering of the reaction between epoxy and amine by the presence of MWCNTs.

The ratio of the loss modulus to the storage modulus is measured as tan δ. The tan δ against temperature plots is given in Figure 4(c). For neat epoxy, there exists a well-defined tan δ relaxation peak centred at 212°C, which is ascribed to the glass transition temperature (T_g) of the cured epoxy resin. The blend and hybrid composites exhibit two tan δ relaxation peaks corresponding of epoxy rich (around 200°C) phase and thermoplastic rich phase (near 110°C).

The tan δ peak heights, peak widths at half-height, and peak areas are summarized in Table III. The tan δ peak height for cross-linked blend and hybrid composites are found to be higher than for the unmodified amine-cross-linked epoxy resin. The increase in the height of the tan δ peak of hybrid composites is associated with changes in the crosslink density. The addition of the thermoplastic and MWCNTs to the epoxy monomer reduces the crosslinking degree attained by the polymer matrix, which results in higher segmental mobility at the T_g; hence, the peak height increases.[45]

The molecular weight between the crosslinks (M_c), which is an indirect measure of crosslink density of epoxy resin, can be calculated from the T_g of epoxy rich phase using the following equation.[46]

$$M_c = \frac{3.9 \times 10^4}{T_g - T_{g0}} \tag{6}$$

where T_g is the glass transition temperature of the crosslinked epoxy resin and T_{g0} is the glass transition temperature of uncrosslinked polymer having same composition as crosslinked polymer. The value of T_{g0} was taken as 91°C for DGEBA/DDS system.[47] The effective crosslink density (υ_e) was calculated from M_c using the following equation.[46]

$$\upsilon_e = \frac{\rho N_A}{M_c} \tag{7}$$

where ρ is the density and N_A is Avogadro's number.

The molecular weight between the crosslinks (M_c) and the effective crosslink density (υ_e) are summarized in Table III. The increase in M_c and consequent decrease in crosslink density for hybrid composites is evident from the table.

Thermal Expansion Behavior

The thermo mechanical analysis (TMA) thermograms of the cured epoxy composites are shown in Figure 5. From the thermograms, the dimensional change increases with increase in temperature. The response of the hybrid composite samples is

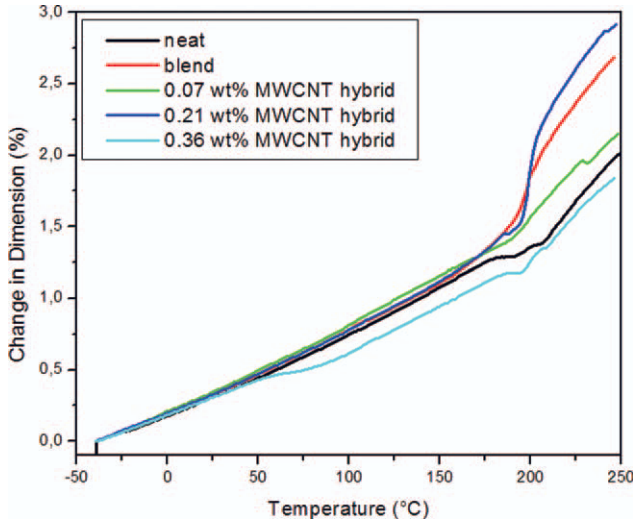

Figure 5. Dimensional change versus temperature plot for neat epoxy, blend, and hybrid composites. [Color figure can be viewed in the online issue, which is available at wileyonlinelibrary.com.]

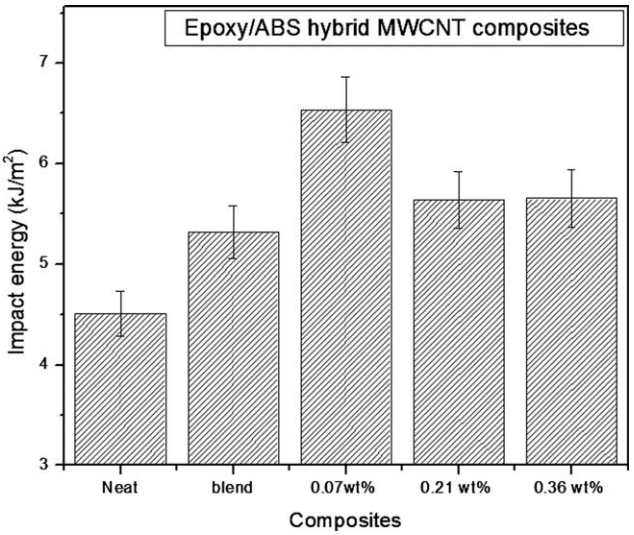

Figure 6. Impact strength of neat epoxy, blend, and hybrid composites.

greater than neat epoxy but is comparable with pure blend. The change in dimension with respect to temperature can be explained by the concept of molecule interaction. With the increase in temperature, molecular vibration in the material increases, which causes an increase in the intermolecular distance.[14] The addition of the thermoplastic and MWCNTs to the epoxy monomer reduces the crosslinking degree attained by the polymer matrix, which results in higher molecular vibration by the application of heat. On the other hand, for 0.36 wt % MWCNTs modified hybrid composites, their might be enough MWCNTs to restrict the mobilization of MWCNTs/epoxy molecules, which limits the amplitude of vibration especially at high temperatures (between 60 and 180°C). During heating, the composites expand and then undergoe a glassy-to-rubbery transformation (T_g); it then continues to expand in the rubbery phase with a greater liner expansion coefficient, showing the normal expansion behaviour of rubber state.

Mechanical Tests

Impact strength of a material describes the energy required to break the specimen under sudden load. The magnitude of the impact strength reflects the ability of the material to resist impact. The Charpy impact tests were carried out for epoxy composites. The impact energies of DDS cured hybrid epoxy/MWCNTs composites are shown in Figure 6. All MWCNTs composites have significantly higher impact strength compared to the neat materials. This indicates a synergetic effect, which shows the capability of both ABS and MWCNTs for the use of high-performance applications. A maximum of around 45% increase in impact strength was achieved with 0.07 wt % MWCNTs respect to epoxy neat epoxy. On the other hand, for 0.21 and 0.36 wt % MWCNTs, the impact strength decreases, because when more MWCNTs are present, the possibility of pull out and debonding between the filler and matrix increased.

Fracture toughness is the resistance of material to crack initiation and propagation. The fracture toughness was expressed as stress intensity factor K_{IC}. Plots of K_{IC} against MWCNTs content in the cured blends are presented in Figure 7. From the figure, it can be seen that fracture toughness of the epoxy resin was improved by the addition of MWCNTs in the blend. A maximum increase of around 56% in K_{IC} was observed with respect to neat crosslinked epoxy system. These results are in according to the literature that is an improvement in toughness was observed (most of the cases) in epoxy hybrid composites.[48–50]

The important factors influencing the fracture toughness are the morphology of the blends, amount of modifier added, the interfacial adhesion between the phases, and the curing conditions.[14] Heterogeneous morphology is very much important for getting improved fracture toughness. Figure 8 reveals the FESEM micrographs of samples observed under microscope after the K_{IC} fracture test. Figure 8(a) reveals the fracture surface of unmodified epoxy resin, which was smooth, with free and regular crack propagation, indicating the characteristics of a brittle

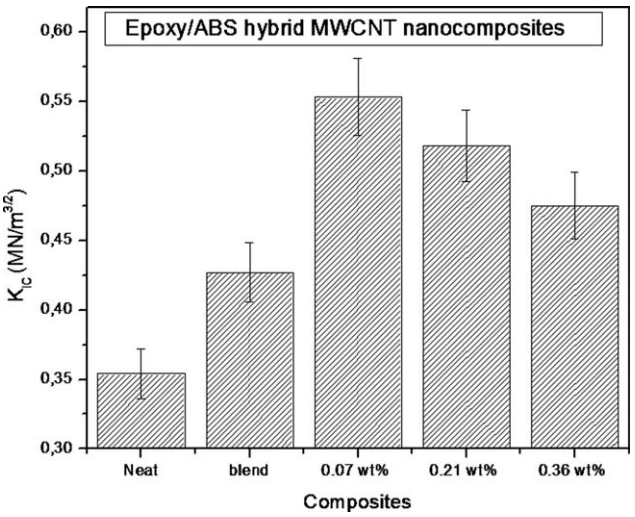

Figure 7. Fracture toughness (K_{IC}) of neat epoxy, blend, and hybrid composites.

Applied Polymer SCIENCE

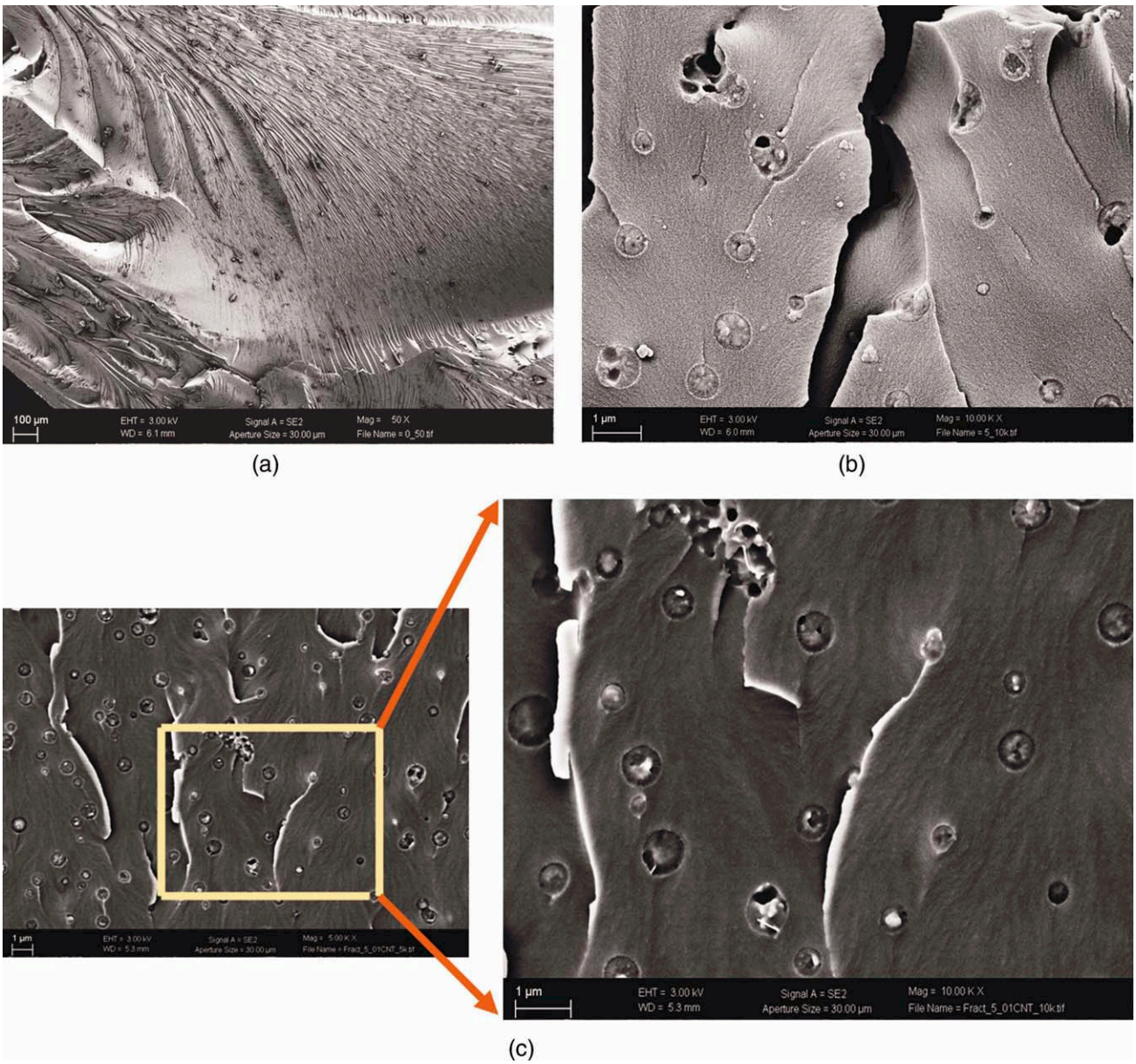

Figure 8. Field emission scanning electron microscopy of failed surfaces of neat epoxy, blend, and hybrid composites. [Color figure can be viewed in the online issue, which is available at wileyonlinelibrary.com.]

material. From our previous studies, we got maximum toughness for 3.6 wt % ABS-modified epoxy blend.[14] The SEM of fractured surface is given in Figure 8(b), revealed the two-phase morphology for the 3.6 wt % ABS-modified epoxy blend. The ABS particles may act as stress concentrators on the application of external load and will lead to ductile tearing of thermoplastic and also plastic deformation of the matrix surrounding the ABS particles. This will contribute to river marks and hence offer more roughness to the fracture surface and hence more ductility to the epoxy matrix. The high degree of roughness on the fractured surface also indicates the crack deviation from its original plane, resulting in an increased surface area of the crack, which may also increase the toughness. Another important factor to be mentioned is the formation of nanocavities around 100 nm during the fracture process. The nanocavities in the ABS domains are very clear from the micrographs; the formation of nanocavities may take up a significant amount of applied stress and hence elevates the fracture toughness. The cavitation process in ABS may be due the presence of rubber content (5 wt %) in ABS phase and is a phenomenon frequently observed in rubber modified epoxy blends.[51]

The fracture surface of the MWCNTs/ABS/epoxy hybrid composites is shown in Figure 8(c–e) as for the epoxy blend the FESEM micrographs for hybrid composites were rougher and presented ductile drawing, plastic deformation, and nanocavitation. The micrographs reveal fracture surfaces with and without MWCNTs. It is quite unpredictable for the localization of MWCNTs in polymer blends, because there are many factors affecting it, such as polarity, viscosity, mixing sequence, phase

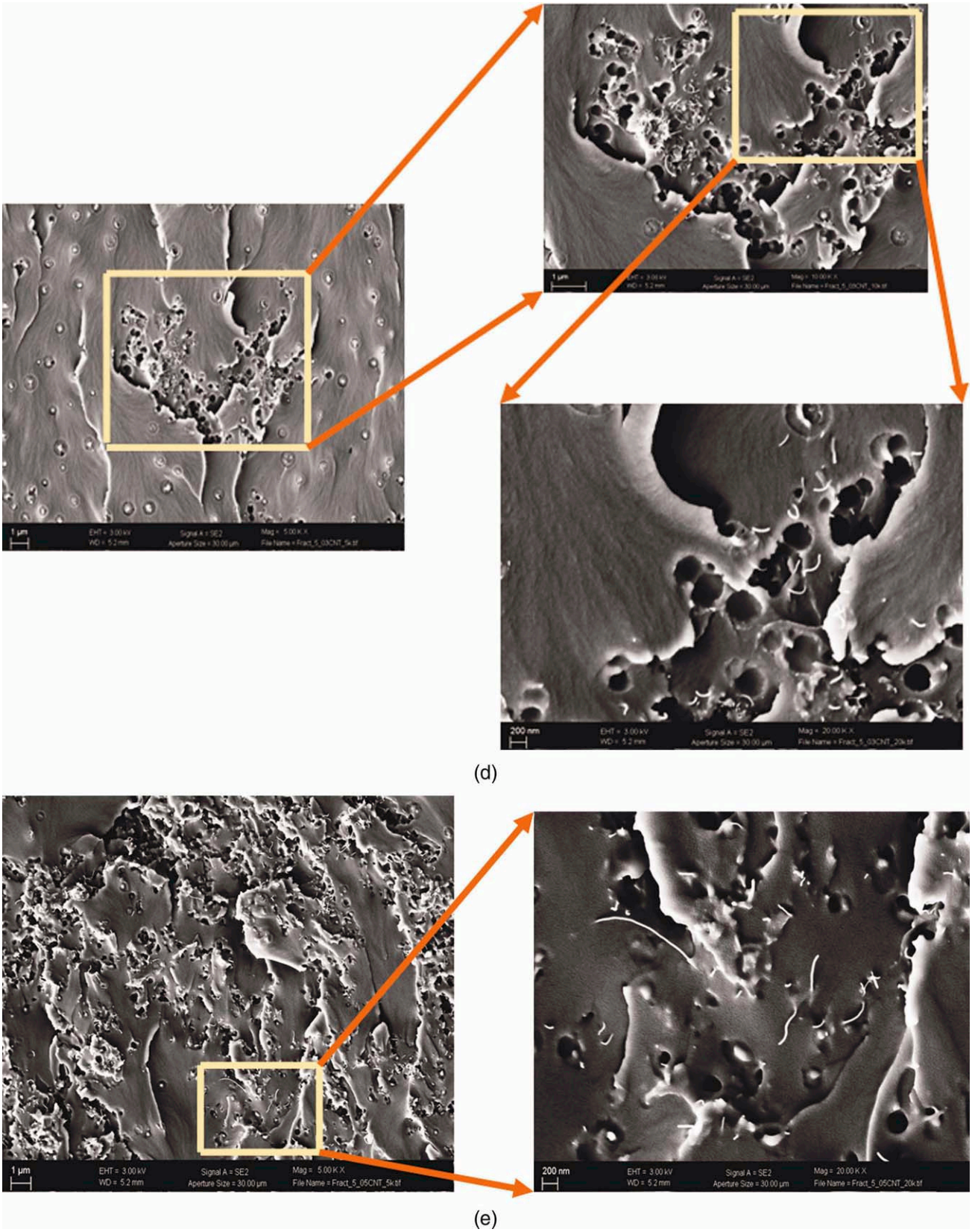

Figure 8. Continued

separation, and so on. Therefore, the MWCNTs might localize in epoxy phase, ABS phase, or both of them. From the micrographs, it can be seen that the carbon nanotubes are fractured, and also some are pulled out of the epoxy matrix but are dispersed in the blend matrix and are separated from one another. Nanotube pull out was observed in all MWCNTs hybrid composites this is understandable given the nonfunctionalized character of the MWCNTs, indicating poor adhesion between the matrix and MWCNTs.[52–54] The presence of MWCNTs enhances the rubber cavitation process, and the dark circles shown in micrographs are considered as rubber particle cavitation. The stress whitening is due to rubber particle cavitation and matrix dilation, is essential to the energy absorbing mechanism, and hence elevates the fracture toughness.[36] Another main toughening mechanism seems to be nanotube pull out, other than caviation are ductile drawing, rivers bands, and plastic deformation.[54] Nanotube pull-out, thermoplastic tearing, and cavitation were largely observed in these composites and were considered to be the main sources of energy dissipation leading to the improved toughness. For 0.21 and 0.36 wt % MWCNTs/ABS/epoxy hybrid composites [Figure 8(d,e)], we observe regions with nonuniform dispersion of thermoplastic domains. In these regions, MWCNTs are selectively dispersed and agglomerated and with extensive thermoplastic cavitations, and these observations increased the possibility of pull out and debonding between the filler and matrix and hence decreased mechanical properties.

CONCLUSION

Thermoplastic modification is an effective way to improve the mechanical and thermal properties epoxy systems. DDS-cured ABS/epoxy blend posses a heterogeneous two-phase structure in which ABS particles were uniformly dispersed in the continuous epoxy matrix. The dynamic mechanical analysis of the blend reveals two T_gs corresponding to epoxy- and ABS-rich phases, which confirms the two-phase morphology in blends. For hybrid composites, MWCNTs localize in epoxy phase, ABS phase, or both of them. From the experimental results, it can be stated that the addition of MWCNTs decreases the rate of the reaction and is reflected in all the properties studied, especially from the decrease in epoxy T_g from the dynamic mechanical analysis (DMA). The improvement in storage modulus by the addition of nanofillers provided better load bearing capacity for the composites. The thermal and dimensional stability of the hybrid composites are comparable with that of neat crosslinked epoxy and the blend. The impact and fracture toughness were significantly improved for the hybrid composites. Nanotube pull out, thermoplastic tearing, and cavitation were largely observed in these hybrid composites and could be the main sources of energy dissipation leading to the improved toughness. To conclude this study reveals potential of "hybrid composites" in composite industry.

ACKNOWLEDGMENTS

The companies Bayer Material Science AG (Leverkusen, Germany), Chi Mei Corporation, Taiwan and Atul Ltd, India are acknowledged for the kind supply of CNT, ABS, epoxy monomer and curing agent. Authors acknowledge instrumental facilities from Leibniz-Institute of Polymer Research Dresden. Authors acknowledge the kind support of Mr.Kunath for taking the SEM and PVT measurements.

REFERENCES

1. Varma, K.; Gupta, V. B. InComprehensive Composite Materials; Elsevier Science: Amsterdam, The Netherlands, **2003;** pp 1–56.
2. Fink, J. K. In Reactive Polymers Fundamentals and Applications; William Andrew: Norwich, NY, **2005**; Chapter 3, pp 139–240.
3. Strehmel, V.; Zimmermann, E.; Häusler, K. -G.; Fedtke, M. *Prog. Colloid Polym. Sci.* **1992,** *90*, 206.
4. Jyotishkumar, P.; Pionteck, P.; Özdilek, C.; Moldenaers, P.; Thomas, S. *Soft Matter* **2011,** *7*, 7248.
5. Mathew, V. S.; Sinturel, C.; George, S. C.; Thomas, S. *J. Mater. Sci.* **2010,** *45*, 1769.
6. Thomas, R.; Abraham, J.; Thomas, P. S.; Thomas, S. *J. Polym. Sci. Part B Polym. Phys.* **2004,** *42*, 2531.
7. Dispenza, C.; Spadaro, G.; Mc Grail, P. T. *Macromol. Chem. Phys.* **2005,** *206*, 393.
8. Mimura, K.; Ito, H.; Fujioka, H. *Polymer* **2000,** *41*, 4451.
9. Francis, B.; Thomas, S.; Asari, G. V.; Ramaswamy, R.; Jose, S.; Rao, V. L. *J. Polym. Sci. Part B Polym. Phys.* **2006,** *44*, 541.
10. Hameed, N.; Sreekumar, P. A.; Thomas, P. S.; Jyotishkumar, P.; Thomas, S. *J. Appl. Polym. Sci.* **2008,** *110*, 3431.
11. Kim, B. S.; Chiba, T.; Inoue, T. *Polymer* **1995,** *36*, 43.
12. Almen, G.; Byrens, R. M.; Mackenzie, P. D.; Maskell, R. K.; McGrail, P. T.; Sefton, M. S. *In 34th International SAMPE Symposium,* **1989,** *34*, 259.
13. Girard–Reydet, E.; Vicard, V.; Pascault, J. P.; Sautereau, H. *J. Appl. Polym. Sci.* **1997,** *65*, 2433.
14. Jyotishkumar, P.; Pionteck, J.; Häßler, R.; George, S.; Cvelbar, U.; Sabu, T. *Ind. Eng. Chem. Res.* **2011,** *50*, 4432.
15. Hodgkin, J. H.; Simon, G. P.; Varley, R. *J. Polym. Adv. Technol.* **1998,** *9*, 3.
16. Pinnavaia, G. B.; John Wiley & Sons: New York, **2000**; Chapter 7, p 127.
17. Dispenza, C.; Carter, J. T.; McGrail, P. T.; Spadaro, G. *Polym. Int.* **1999,** *48*, 1229.
18. Balakrishnan, S.; Raghavan, D. *Macromol. Rapid Commun.* **2004,** *25*, 481.
19. Spitalsky, Z.; Tasis, D.; Papagelis, K.; Galiotis, C. *Prog. Polym. Sci.* **2010,** *35*, 357.
20. Monthioux, M.; Kuznetsov, V. L. *Carbon* **2006,** *44*, 1621.
21. Zhang, M.; Li, J. *Mater. Today* **2009,** *12*, 12.
22. Lu, J. P. *Phys. Rev. Lett.* **1997,** *79*, 1297.
23. Sandler, J.; Shaffer, M. S. P.; Prasse, T.; Bauhofer, W.; Schulte, K.; Windle, A. H. *Polymer* **1999,** *40*, 5967.
24. Xiao, L.; Chen, Z.; Feng, C.; Liu, L.; Bai, Z. Q.; Wang, Y.; Li, Q.; Zhang, Y.; Li, Q.; Jiang, K.; Fan, S. *Nano Lett.* **2008,** *8*, 4539.

25. New Flexible Plastic Solar Panels Are Inexpensive And Easy To Make. Science Daily. July 19, **2007**. Available at: http://www.sciencedaily.com/releases/2007/07/070719011151.htm.
26. Simmons, T.; Hashim, D.; Vajtai, R.; Ajayan, P. M. *J. Am. Chem. Soc.* **2007,** *33*, 10088.
27. Logakis, E.; Pandis, C.; Peoglos, V.; Pissis, P.; Charalampos, S.; Pionteck, J.; Potschke, P.; Micusik, M.; Omastova, M. *J. Polym. Sci. Part B Polym. Phys.* **2009,** *47*, 764.
28. Logakis, E.; Pandis, C.; Peoglos, V.; Pissis, P.; Pionteck, J.; Potschke, P.; Micusik, M.; Omastova.M. *Polymer* **2009,** *50*, 5103.
29. Logakis, E.; Pollatos, E.; Pandis, C.; Peoglos, V.; Zuburtikudis, I.; Delides, C. G.; Vatalis, A.; Gjoka, M.; Syskakis, E.; Viras, K.; Pissis, P. *Comp. Sci. Technol.* **2010,** *70*, 328.
30. Gojny, F. H.; Wichmann, M. H. G.; Kopke, U.; Fiedler, B.; Schulte, K. *Compos. Sci. Technol.* **2004,** *64*, 2363.
31. Sui, G.; Zhong, W. H.; Liu, M. C.; Wu, P. H. *Mater. Sci. Eng. A* **2009,** *512*, 139.
32. Fröhlich, J.; Thomann, R.; Mülhaupt, R. *Macromolecules* **2003,** *36*, 7205.
33. Marouf, B. T.; Pearson, R. A.; Bagheri, R. Mater. Sci. Eng. *A* **2009,** *515*, 49.
34. Hernandez, M.; Sixou, B.; Duchet, J.; Sautereau, H. *Polymer* **2007,** *48*, 4075.
35. Park, J. H.; Jana, S. C. *Polymer* **2003,** *44*, 2091.
36. Liang, Y. L.; Pearson, R. A. *Polymer* **2010,** *51*, 4880.
37. Jyotishkumar, P.; Häußler, L.; Pionteck, J.; Adam, G.; Thomas, S. *J. Macro Sci. Part B Phys.* Doi: 10.1080/00222348.2011.629853.
38. Jyotishkumar, P.; Logakis, E.; Pionteck, J.; Häussler, L.; Haßler, R.; Pissis, P.; Thomas. S. *J. Appl. Polym. Sci., in press.*
39. Guadagno, L.; Vertuccio, L.; Sorrentino, A.; Raimondo, M.; Naddeo, C.; Vittoria, V.; Iannuzzo, G.; Calvi, E.; Russo, S. *Carbon* **2009,** *47*, 2419.
40. Don, T. M.; Bell, J. P. *J. Appl. Polym. Sci.* **1998,** *69*, 2395.
41. Tao, K.; Yang, S.; Grunlan, J. C.; Kim, Y. S.; Dang, B.; Deng, Y. *J. Appl. Polym. Sci.* **2006,** *102*, 5248.
42. Kim, S. H.; Lee, W.; Park, J. M. *Carbon* **2009,** *47*, 2699.
43. Hameed, N.; Sreekumar, P. A.; Valsaraj, V. S.; Thomas, S. *Polym. Compos.* **2009,** *30*, 982.
44. Mathew, V. S.; Jyotishkumar, P.; George, S. C.; Gopalakrishnan, P.; Delbreilh, L.; Saiter, J. M.; Saikia, P. J.; Thomas, S. *J. Appl. Polym. Sci.* **2012,** *125*, 804.
45. Jyotishkumar, P.; Koetz, J.; Tiersch, B.; Strehmel, V.; Özdilek, C.; Moldenaers, P.; Hässler, R.; Thomas, S. *J. Phys. Chem. B* **2009,** *113*, 5418.
46. Nielsen, L. E. *J. Macromol. Sci. Rev. Macromol. Chem.* **1969,** *3*, 69.
47. Bellenger, V.; Verdu, J.; Morel, E. *J. Polym. Sci. Part B: Polym. Phys.* **1987,** *25*, 1219.
48. Gam, K. T.; Miyamoto, M.; Nishimura, R.; Sue, H. *J. Polym. Eng. Sci.* **2003,** *43*, 1635.
49. Fröhlich, J.; Thomann, R.; Mülhaupt, R. *Macromolecules* **2003,** *36*, 7205.
50. Fröhlich, J.; Thomann, R.; Gryshchuk, O.; Kocsis, J. K.; Mülhaupt, R. *J. Appl. Polym. Sci.* **2004,** *92*, 3088.
51. Bubeck, R. A.; Buckley, D. J.Jr.; Karmer, E. J.; Brown, H. R. *J. Mater. Sci.* **1991,** *26*, 6249.
52. Breton, Y.; Desarmot, G.; Salvetat, J. P.; Delpeux, S.; Sinturel, C.; Beguin, F.; Bonnamy, S. *Carbon* **2004,** *42*, 1027.
53. Song, Y.; Youn, J. R. *Carbon* **2005,** *43*, 1378.
54. Wichmann, M. H. G.; Schulte, K.; Wagner, H. D. *Compos. Sci. Technol.* **2008,** *68*, 329.